



AIR-BORNE TIE-SONAR FOR LOADED TIE DEFLECTION MEASUREMENTS

SUMMARY

This report presents a non-contact ultrasonic technique to map the full-field surface deflection of railroad ties using known concepts of sonar-based distance measurements. Between September 2019 and July 2021, the University of California San Diego (UCSD) created a beam with six sonar sensors and performed field testing at the UCSD Rail Defect Testing Facility (RDTF) and at a Burlington Northern Santa Fe (BNSF) rail yard in San Diego, CA. The test results indicate the potential of this non-contact system to measure full-field tie deflections in three-dimensions (3D) and possibly detect defective tie-ballast support conditions such as center-binding.

BACKGROUND

Degraded tie support conditions can lead to premature failure of ties, gage widening, and other issues that can lead to derailments. Voids in the tie-ballast interface near the ends of the tie are the primary cause of center-binding support conditions [1]. The Volpe National Transportation Systems Center (Volpe) conducted a study that shows how the detection of deteriorated support conditions such as center-binding or negative flexural bending is possible through measurements of vertical deflection profiles of the ties [2].

The deflected profile of a loaded tie can provide useful information related to the quality of the ballast layer supporting the tie. Traditional ballast quality measurement methods are manual techniques that disturb the ballast layer. Measuring a tie deflection under load may be a surrogate for traditional methods and measuring tie deflection at speed would greatly increase the efficiency of inspection.

OBJECTIVES

The objective of this research was to develop a non-contact measurement system to record the deflected profile of crossties under load while moving along the track. The effort was limited to a proof of concept with testing at UCSD laboratories and BNSF field locations.

METHODS

UCSD's measurement system uses an array of capacitive ultrasonic transducers arranged along the longitudinal axis of the ties at a lift-off distance of 3 inches from the rail surface to ensure contactless measurements (Figure 1).

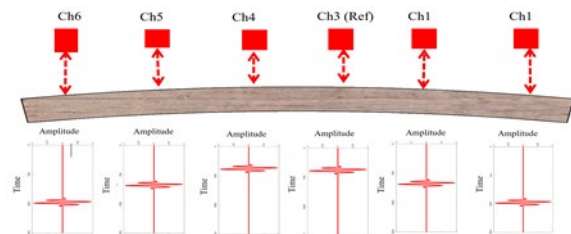


Figure 1 - Schematic diagram of transducer array and corresponding waveforms for tie with center-binding

The technique uses a pulse-echo mode with a transducer array to measure the distances from the transducers to the tie by tracking the time-of-flight of the ultrasonic waves reflected from the tie surface. The same transducer receives the transmitted acoustic signal reflected by the top surface of the tie. Knowing the speed of sound in air ($v = 343$ m/sec), the distance of the tie surface from the transducer face, d , can be calculated as:

$$d = \frac{t \times v}{2} \quad (1)$$



where t is the arrival time (time-of-flight) of the reflected wave from the tie surface. The factor of 2 considers the distance travelled by the wave from the transducer to the tie surface and back.

The system uses an acoustic signal strength-based technique to differentiate between signals reflected from ties and ballast based on the wave scattering phenomenon. Multiple measurements along the tie width enable the system to measure lateral (twisting) deformations of the tie section along with longitudinal deformations (3D deflections).

Figure 1 shows the assumed deflected shape of the tie due to wheel loads. The distance between Ch1 to the tie surface is greater than the distance between Ch3 to the tie surface. Therefore, the corresponding wave packet in Ch3 arrives earlier than Ch1. Computing the distance from the tie surface at each channel can be done by tracking the time-of-flight and using Equation (1). However, this measurement does not directly yield the displacement at that transducer location.

The team developed a reference-based cross-correlation operation to compute the time-of-flight with one of the transducers used as a reference for the distance measurements. The difference in time-of-flight (Δt) is proportional to the deflection at Ch1 with respect to Ch3. To compute Δt , consider $x_1(t)$ as the time-series signal at Ch1 and $x_3(t)$ as the time-series signal at Ch3. The cross-correlation operator $R_{31}(\tau)$ is:

$$R_{31}(\tau) = \sum_{t=0}^{t=T} x_3(t) x_1(t - \tau) \quad (2)$$

The difference in time-of-flight Δt can be calculated as:

$$\Delta t = \operatorname{argmax} \{R_{31}(\tau)\} \quad (3)$$

The research team computed the deflection at each transducer location as:

$$\Delta d = \frac{\Delta t \times v}{2} \quad (4)$$

The signal is gated between 1.25 and 2.25 ms, the time window when the reflected signal is

expected. In addition, the signal passes through a Butterworth high pass filter with a cut-off frequency of 10 kHz to eliminate low frequency noise.

The system employed a camera to view the track surface. UCSD developed a machine learning-based technique to discriminate between tie and ballast images and employed the Kanade-Lucas-Tomasi (KLT) algorithm to track features in two successive images. This method eliminated the need for an encoder for system triggering during the BNSF yard test.

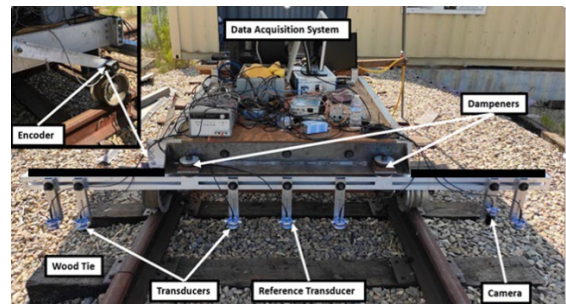


Figure 2 - Test setup with data acquisition system at UCSD's RDTF

The research team conducted tests at walking speeds at UCSD RDTF using a pushcart and at a BNSF rail yard facility using a loaded freight car, Figure 2 and Figure 3.

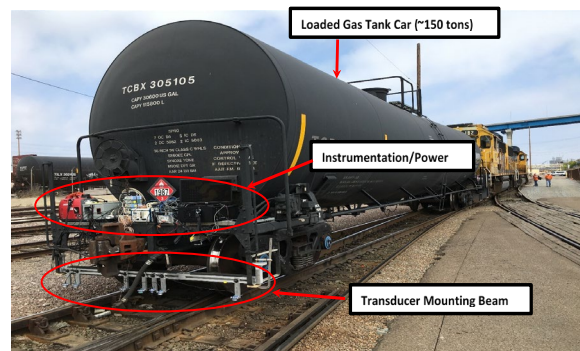


Figure 3 - Test setup at BNSF yard with system mounted on loaded gas tank car

RESULTS

Figure 4 shows the longitudinal and transverse (twisting) deflection results from a tie in one test



run at the BNSF yard. The deflections are scaled by 20x for better visualization. It is clear that the system captures both the longitudinal deflections and the tie twisting deformations from multiple measurements along the tie surface.

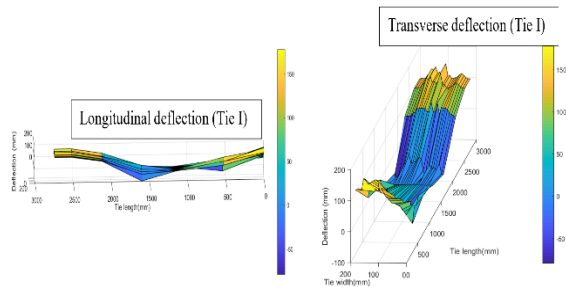


Figure 4 - Longitudinal and transverse (twisting) deformations of a tie (BNSF yard test)

Figure 5 shows deflections from two different test runs over the same tie at the BNSF yard. The similarity in the deflection profiles obtained in different test runs indicates the consistency of the measurements.

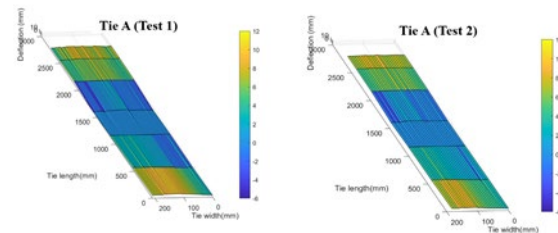


Figure 5 - 3D deflection profiles of same tie in two independent test runs (BNSF yard test)

To test the accuracy of the system, the research team placed a wood spacer of 23 mm thickness on one of the ties. Figure 6 shows the reconstructed surface profile. Figure 7 shows the profile along the tie width. UCSD calculated the true height by subtracting the baseline tie surface elevation from the elevation at the wood plank. This value was found to be equal to the thickness of the wood spacer (23 mm), confirming the distance measurement accuracy.

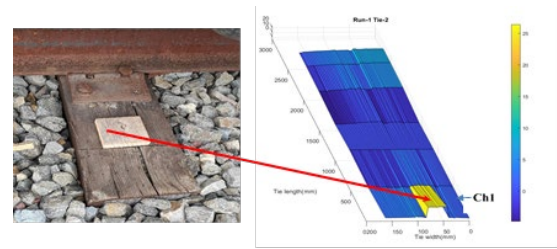


Figure 6 - Reconstructed profile with block of known thickness (23 mm) (BNSF yard test)

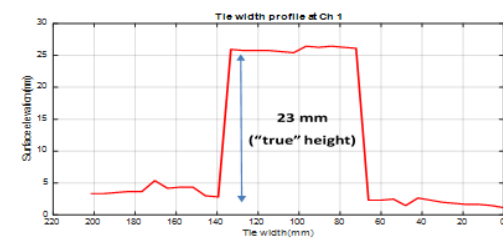


Figure 7 - Tie width profile for tie with wood spacer (BNSF yard test)

UCSD performed a statistical analysis to evaluate the repeatability of the deflection measurements for different runs. The team tracked the tie deflections at each of the two ends with respect to the center for 20 ties and computed the mean and the standard deviation of the tie end deflections over four different test runs. The standard deviation results for most of the ties are less than 1 mm, with a maximum standard deviation of 1.8 mm recorded for tie 18. These results indicate a reasonable level of repeatability with the technique.

CONCLUSIONS

The results from the tests confirm the ability of the technique to measure tie deflection under load at walking speeds with reasonable accuracy and repeatability. The low testing speed provided a measurement at least every 0.25 inches across the width of each tie. At revenue speeds (~ 60 mph) the research team expects approximately five measurements (about every 1.4 inches) across the width of each tie. In conclusion, the technique has the potential to accurately capture loaded tie deflections at speed.



FUTURE ACTION

Some challenges that need to be addressed in future research include 1) the identification of ties misaligned with the transducer array; 2) the need for controls to autonomously identify ties with center-binding; and 3) a full demonstration at revenue speeds that includes mechanical vibrations and acoustic noise.

REFERENCES

- [1] Yu, H., et al., "Failure analysis of railroad concrete cross-ties in the center negative flexural mode using finite element method," in *Proceedings of the Institution of Mechanical Engineers, Part F: Journal of Rail and Rapid Transit*, Cambridge, MA, 2017.
- [2] Yu, H., "[Estimating Deterioration in the Concrete Tie-Ballast Interface Based on Vertical Tie Deflection Profile: A Numerical Study](#)," U.S. Department of Transportation, Report No. JRC2016, Columbia, SC, 2016.

ACKNOWLEDGEMENTS

Special thanks to FRA Program Manager Cameron Stuart for overall guidance and oversight; Ted Sussmann from Volpe for research insights; Robert Banister and Ross Curtright from BNSF for organizing and supporting the field tests in San Diego, CA.

CONTACT

Cameron Stuart

Program Manager
Federal Railroad Administration
Office of Research, Development and
Technology
1200 New Jersey Avenue, SE
Washington, DC 20590
(202) 306-5326
cameron.stuart@dot.gov

Francesco Lanza di Scalea, Ph.D.

Professor of Structural Engineering
Director, Exp. Mech. & NDE Laboratory
University of California, San Diego
9500 Gilman Drive, Mail Code 0085
La Jolla, CA 92093-0085
Tel: 858-822-1458
flanza@ucsd.edu

KEYWORDS

Non-destructive evaluation, ultrasonic inspection, railroad tie deflection, non-contact inspection, ultrasonic ranging, center-binding, track

CONTRACT NUMBER

693JJ619C000019

Notice and Disclaimer: This document is disseminated under the sponsorship of the United States Department of Transportation in the interest of information exchange. Any opinions, findings and conclusions, or recommendations expressed in this material do not necessarily reflect the views or policies of the United States Government, nor does mention of trade names, commercial products, or organizations imply endorsement by the United States Government. The United States Government assumes no liability for the content or use of the material contained in this document.